(Received 10 June 2024, Accepted 16 July 2024, Scheduled 27 July 2024)

Low Profile UHF-RFID Reader Antenna with High Front-to-Back Ratio

Safia Chenaoui[1,*], Lila Mouffok[1], and Sami Hebib[2]

[1] *Aeronautical Sciences Laboratory, Institute of Aeronautics and Spatial Studies, University of Blida 1, Algeria*
[2] *DIC Laboratory, Faculty of Technology, University of Blida 1, Algeria*

ABSTRACT: In this paper, a low profile UHF-RFID reader antenna with high front-to-back ratio is presented. The antenna consists of a probe-fed U-slot rectangular patch antenna loaded with a slotted AMC reflector, formed of 2×2 unit cells. By incorporating the AMC reflector, a compact profile height of 0.049λ (λ is the wavelength at 910 MHz) is achieved with high gain and front-to-back ratio. The proposed reader antenna is fabricated and measured. The experimental results are similar to those predicted by electromagnetic simulation and validate the proper operation of the antenna across the entire UHF-RFID band (860–960 MHz). Moreover, the realized prototype exhibits a measured realized gain and a front-to-back ratio (F/B) greater than 5 dBi and 24 dB, respectively. The proposed design offers the advantages of low profile, high gain and F/B ratio, rendering it suitable for compact RFID readers.

1. INTRODUCTION

With the extensive proliferation of wireless communication devices into modern life, including mobile phones, tablets, internet of things (IoT) devices, and radio-frequency identification (RFID) systems, the importance of the antennas is steadily on the rise. The antennas serve as the crucial link between these devices and the transmission or reception of signals, thereby directly influencing their overall performances. Hence, the careful design of antennas remains a critical aspect in meeting the demands of modern wireless connectivity. Printed patch antennas are often considered as promising candidates for UHF-RFID readers [1–4], due to their attractive characteristics, such as light weight, low cost, and easy fabrication. However, they are constrained by limited input impedance bandwidth [5]. Numerous techniques have been employed to mitigate this drawback, including the insertion of air layers [6, 7], using thick substrates [8, 9], engraving slots in the metallic patch [10], adding parasitic elements [11], creating defects in the ground plane [12], and combining multiple techniques from those previously mentioned [13–15]. Generally, the application of these techniques alters certain antenna characteristics such as gain and front-to-back ratio (F/B ratio), or results in thicker antenna structures. Recently, Artificial Magnetic Conductor (AMC) reflectors provide an alternative solution to enhance antenna characteristics [16, 17] or reduce its overall size [18–20]. These periodic structures with distinct electromagnetic property (in-phase reflection) exhibit a high surface impedance property, which can effectively suppress surface waves [21]. This property contributes to an increase in the antenna broadside gain while simultaneously reducing backward radiation, resulting in a high F/B ratio. Several AMC backed UHF-RFID reader antennas have been proposed in the literature [22–26]. In [22], a dual-band antenna loaded with a dual-band AMC reflector is designed for RFID readers. The proposed antenna is intended to cover the North American UHF-RFID band (902–928 MHz), centered at 915 MHz as well as the popular WLAN band centered at 2.45 GHz. The combined structure has an overall thickness of 30 mm (0.09λ: λ is the wavelength at 915 MHz) and average gains of 3.6 dBi with high F/B ratio of 20 dB at both central frequencies 915 MHz and 2.45 GHz, respectively. In [23], an electromagnetic band gap (EBG) reflector is positioned beneath a UHF-RFID reader antenna to enhance its F/B ratio. The antenna shows a reduced thickness of 0.012λ. Consequently, the property of a high F/B ratio is achieved through the suppression of surface wave propagation by the EBG reflector. The designed antenna demonstrates a maximum gain and high F/B ratio of 6 dBi and 29 dB at 915 MHz, respectively. In addition, a high impedance surface (HIS) structure is loaded on the back of an RFID antenna, reported in [24]. The resulting structure leads to a maximum gain of 6.5 dBi with an F/B ratio of 20 dB at 920 MHz. Further, in [25], a dual band (915 and 2450 MHz) crossed-dipole loaded with an AMC reflector of 8×8 array is investigated for UHF-RFID applications. The proposed structure demonstrates an overall thickness of 40 mm (0.1λ) with a high gain of 8 dBi and F/B ratio of 20 and 25 dB at 915 MHz and 2.45 GHz, respectively. However, most of the previously detailed AMC backed UHF-RFID reader antenna solutions feature thick profile and do not cover the full UHF-RFID band (860–960 MHz).

In this work, a probe-fed U-slot patch antenna backed by a slotted AMC reflector is proposed for UHF-RFID applications. The AMC is positioned beneath the antenna and operates as an electromagnetic wave reflector, serving as an alternative to the conventional ground plane. This configuration reduces the antenna profile, enhances gain and backward radiation perfor-

* Corresponding author: Safia Chenaoui (safiachenaoui@outlook.fr).

mance. Indeed, the resulting structure demonstrates high measured gain (between 5 and 7.90 dBi) and F/B ratio (between 24 and 31 dB) across the entire UHF-RFID band (860–960 MHz), all while maintaining a reduced thickness of only 0.049λ.

This paper is organized as follows. The design methodology of the antenna over the slotted AMC is highlighted in Section 2. Both simulated and measured results are thoroughly discussed in Section 3, and finally a conclusion is drawn in Section 4.

2. U-SLOT PATCH ANTENNA LOADED WITH SLOTTED AMC REFLECTOR

The proposed probe-fed U-slot patch antenna loaded with a slotted AMC reflector is depicted in Fig. 1(a). The U-slot rectangular patch (see Fig. 1(b)) is printed on a 1.6 mm-thick FR4 substrate with a relative permittivity of 4.3 and a loss tangent of 0.025. It is fed by a coaxial probe, extended from the center of the $200 \times 200\,\text{mm}^2$ AMC ground plane to the center of the U-slot patch antenna. The dimensions of the radiating element are (unit: mm): $L_g = 200$, $W_g = 200$, $L_P = 115$, $W_P = 164.7$, $L_S = 43$, $W_S = 80$, $a = 7.94$, and $b = 10.6$. The required wide frequency bandwidth (860–960 MHz) of the structure is achieved by cutting a U-slot in the patch and inserting air layer between the U-slot patch antenna and its AMC reflector. This 10 mm-thick air layer is maintained by four plastic blots.

As shown in Fig. 1(c), the proposed AMC reflector is composed of 2×2 unit cells, printed on a 4.8 mm-thick FR4 dielectric substrate with a relative permittivity of 4.3 and a loss tangent of 0.025. Fig. 2(a) shows the suggested AMC unit cell geometry, which is designed based on a square patch with three parallel longitudinal slots. The right and left longitudinal slots have identical dimensions (length and width), while the middle slot maintains the same width but differs in length. These

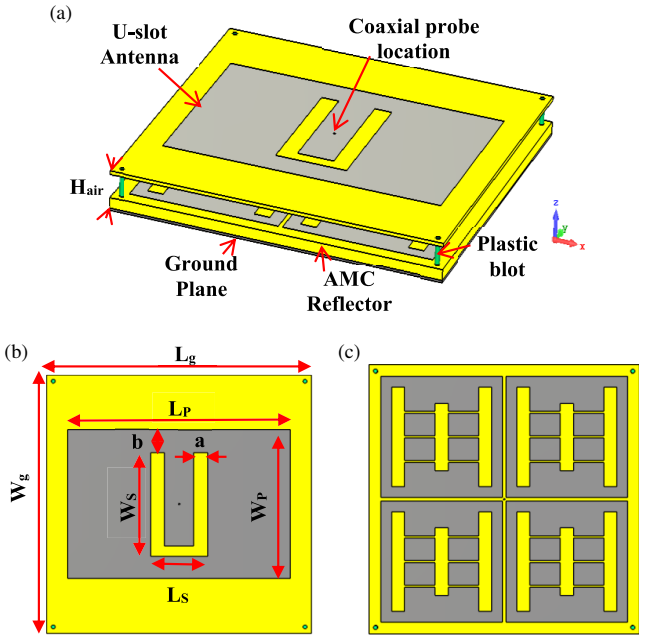

FIGURE 1. Geometry of the proposed U-slot patch antenna over the slotted AMC reflector. (a) Overall antenna structure. (b) Geometry of the proposed U-slot patch antenna. (c) AMC reflector top view.

three longitudinal slots are perpendicularly crossed by three other identical parallel transverse slots, collectively forming a ladder-shaped slot configuration. The main purpose of slotting the AMC surfaces is to increase the equivalent inductance and consequently reduce the resonance frequency. The dimensions of the proposed AMC unit cell are (unit: mm): $L_{\text{cell}} = 67.5$, $W_{\text{AMC}} = 57.5$, $W_A = 49$, $L_A = 8$, $W_B =, 2$, $W_D = 2.5$, $L_C = 35$, and $W_C = 10$.

The reflection phase property of the AMC surface is obtained by modeling and simulating its single unit cell with CST Microwave Studio software. As illustrated in Fig. 2(b), a single AMC unit cell is placed under a radiating electromagnetic box using periodic boundary conditions, with the four walls set as Perfect Electric Conductor (PEC) and Perfect Magnetic Conductor (PMC). The AMC unit cell is excited by a wave port in order to generate a normal incident electromagnetic wave. It can be seen from the simulated data presented in Fig. 2(c) that the in-phase reflection bandwidth ($\pm 90°$) of the designed AMC unit cell ranges from 890 MHz to 924 MHz (blue-highlighted area) with a resonance frequency of 910 MHz.

Figure 3 shows the variation of the F/B ratio versus frequency of the designed U-slot patch antenna with/without the AMC reflector. It can be noted that the F/B ratio is significantly increased after the incorporation of the AMC reflector while maintaining quite similar gain performance. The AMC backed antenna shows an F/B ratio varying between 23.6 and 32.46 dB across the full UHF-RFID band, whereas it ranges between 15.5 and 18 dB for the U-slot patch antenna without the AMC reflector. Otherwise, the realized gain experiences a slight decrease of 1 dBi across the full UHF-RFID band (varying between 6 and 7.67 dBi) compared to the design without the AMC reflector (6.80–7.88 dBi). The antenna exhibits a high F/B ratio, demonstrating the ability of the AMC surface to suppress backward radiation when being used as an antenna reflector. It is worth noting that the antenna without an AMC reflector requires an air layer of 26.8 mm (10 mm with AMC) between the antenna and its ground plane to cover the entire UHF-RFID band. This highlights the effectiveness of AMC surface not only in enhancing F/B ratio but also in reducing the antenna thickness.

A parametric study is conducted to investigate the impact of the H_{air} on the AMC backed U-slot patch antenna performances. Fig. 4 and Fig. 5 illustrate the effect of this key parameter on the reflection coefficient, realized gain, and F/B ratio. It can be observed that the impedance matching deteriorates as the air layer thickness decreases, particularly at 900 MHz when $H_{\text{air}} = 6$ mm. This degradation causes dips in the realized gain, reaching approximately 1.78 dBi with an F/B ratio of 28 dB.

However, for the other values of H_{air}, the antenna exhibits good impedance matching across the UHF-RFID frequency band (860–960 MHz) (see blue highlighted area) with high realized gain and F/B ratio. The realized gain varies between 5.11–7.54 dBi, 6–7.67 dBi, and 6.29–7.76 dBi, while the F/B ratio ranges between 24–34 dB, 23.6–32.46 dB, and 22–26.8 dB for $H_{\text{air}} = 8$, $H_{\text{air}} = 10$ mm, and $H_{\text{air}} = 12$ mm, respectively. Finally, an air layer thickness of 10 mm is selected as an optimal tradeoff among impedance matching, gain, F/B ratio, and structure thickness.

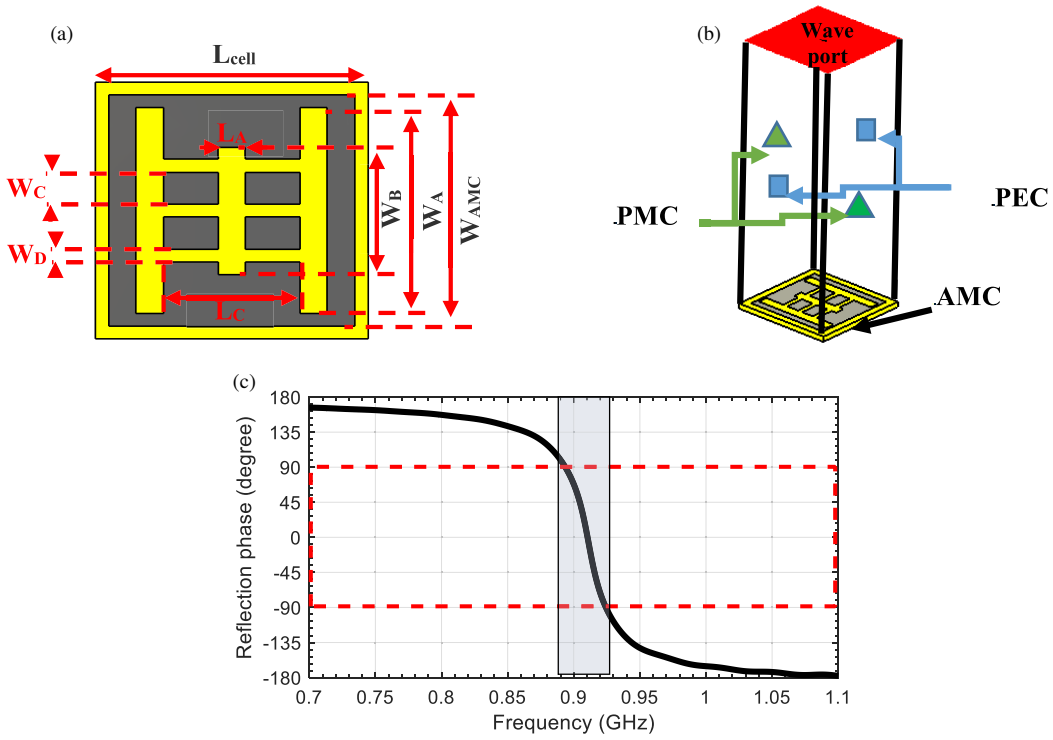

FIGURE 2. The proposed AMC unit cell and its reflection phase response. (a) AMC unit cell geometry. (b) Its electromagnetic mode. (c) Reflection phase response.

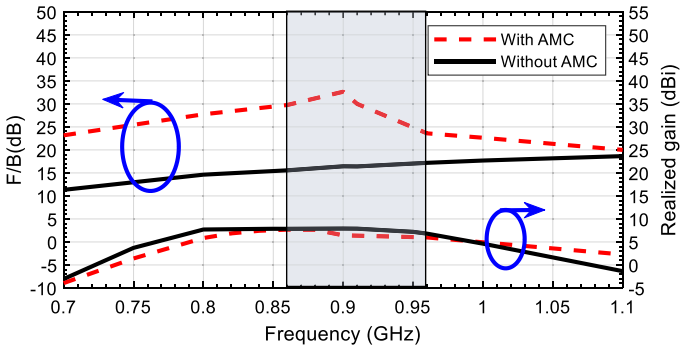

FIGURE 3. Simulated realized gain and front-to-back ratio of the proposed U-slot patch antenna with/without AMC reflector.

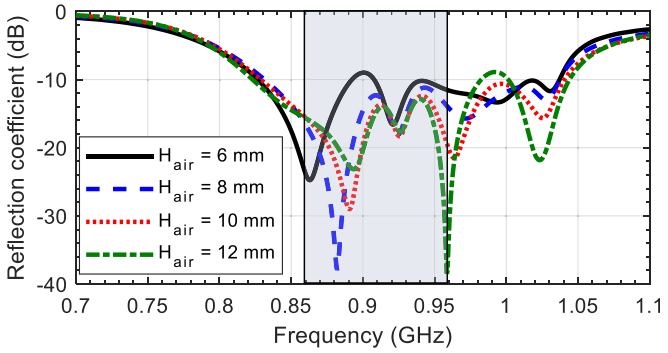

FIGURE 4. Effect of the air layer thickness on the resulting structure reflection coefficient.

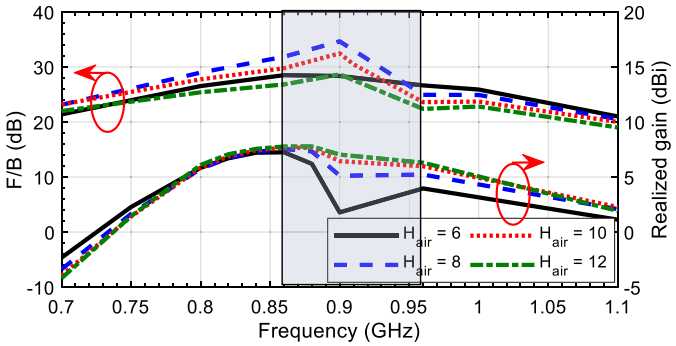

FIGURE 5. Effect of the air layer thickness on the realized gain and F/B ratio of the proposed AMC-backed U-slot patch antenna structure.

The surface current distribution on the AMC reflector is plotted in Fig. 6, at three distinct frequencies: 860 MHz, 910 MHz, and 960 MHz. It can be obviously seen that there is no current distribution on the AMC surface, except at the frequency of 960 MHz, where slight current concentrates at the middle of the AMC reflector. It is worth noting that the limited current circulation on the AMC reflector plays a crucial role in preventing performances degradation, particularly in terms of radiation, thereby explaining its ability to enhance the F/B ratio.

3. MEASUREMENT RESULTS AND DISCUSSIONS

The proposed U-slot patch antenna backed by the slotted AMC reflector is fabricated and assembled as shown in Fig. 7. The reflection coefficient of the prototype is measured using Keysight Agilent PNA Network Analyzer N5222A. The simulated and measured reflection coefficient results are depicted in Fig. 8(a). A good agreement is observed between simulated and tested

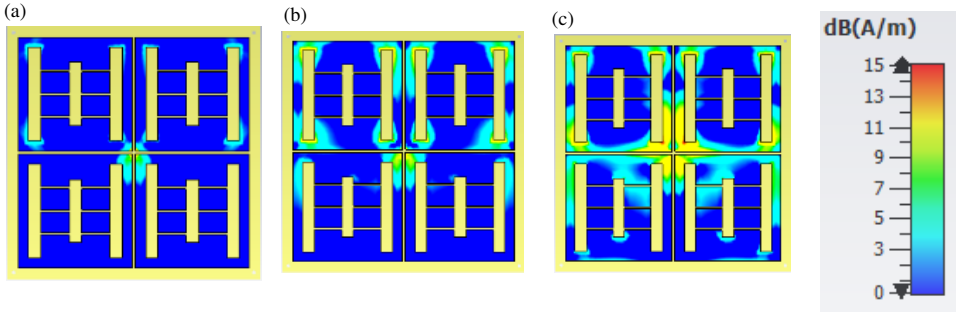

FIGURE 6. Surface current distribution on the AMC surfaces at: (a) 860 MHz, (b) 910 MHz, (c) 960 MHz.

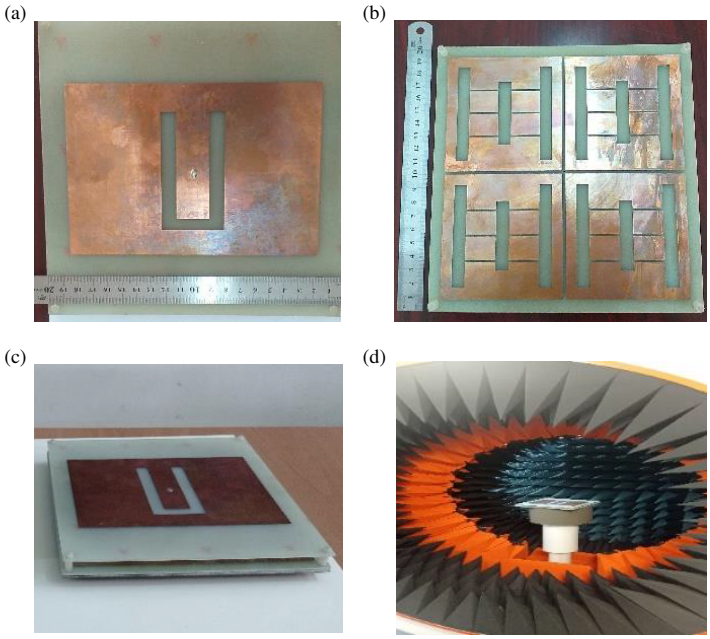

FIGURE 7. Photographs of the fabricated U-slot antenna backed by the slotted AMC reflector and its measurement results. (a) Fabricated U-slot patch antenna. (b) Fabricated 2 × 2 AMC unit cells. (c) Assembled prototype. (d) Measurement setup in the MVG starLab anechoic chamber.

Ref.	Size (mm^3)	BW (MHz)	Gain (dBi)	F/B (dB)
[1]	150 × 150 × 24	846–926	6	22
[3]	150 × 150 × 60	860–866	3	15
[4]	220 × 220 × 27	917–923	6.6	20
[6]	250 × 250 × 35	818–964	8	20
[7]	200 × 200 × 19	855–918	9	20
[8]	250 × 250 × 29.8	835–955	7	20
[13]	150 × 150 × 34	902–928	6	16
[22]	188 × 188 × 30	905–930	3	20
[24]	255 × 255 × 40	844–955	8	20
[26]	150 × 150 × 12	869–936	5	15
This work	200 × 200 × 16.4	860–960	6.36	30

F/B: is provided at the center frequency

TABLE 1. Comparison between the U-slot antenna with RFID reader antennas operating in the UHF band.

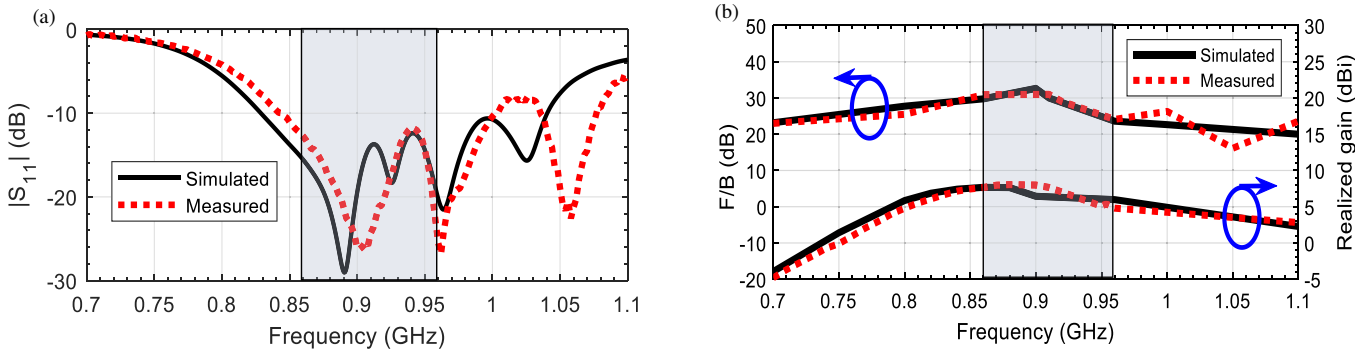

FIGURE 8. Simulated and measured antenna charctersiatics, (a) reflection coefficient, (b) realized gain and F/B ratio.

results, except a slight frequency shift in the band 1–1.1 GHz. The measured impedance bandwidth is 24% (846–1075 MHz), which covers the full UHF-RFID band (860–960 MHz). The radiation pattern measurements of the fabricated prototype have been performed in the StarLab at LCIS laboratory, France. Fig. 8(b) illustrates the simulated and measured realized gains and F/B ratios versus frequency. The comparison shows a good agreement between simulated and measured results, with

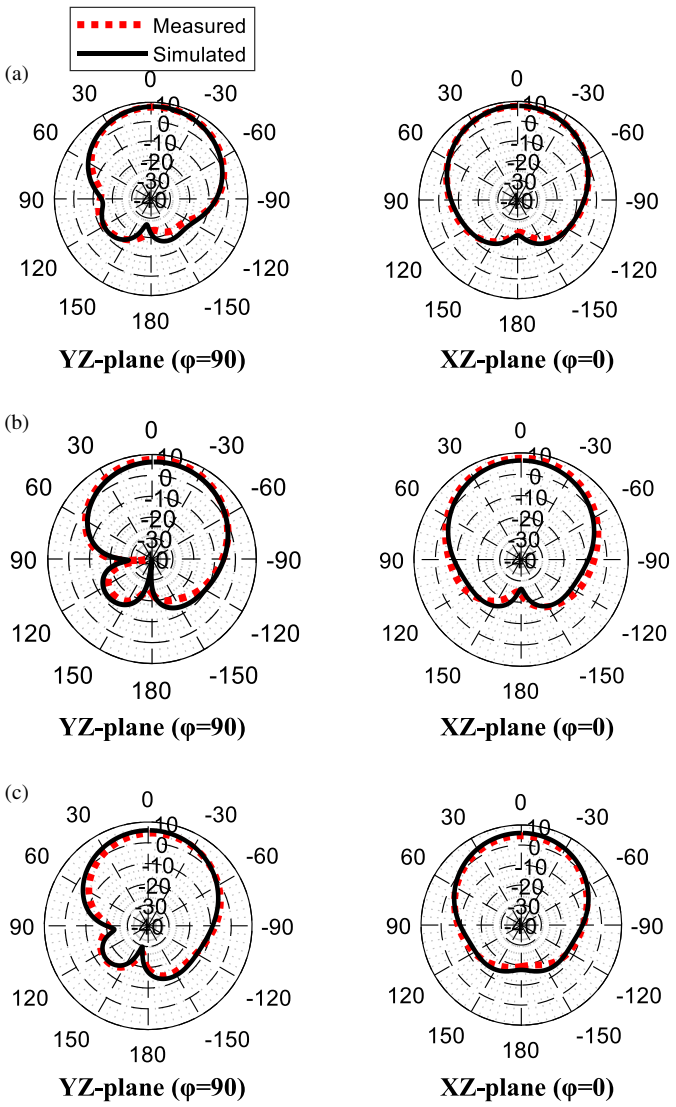

FIGURE 9. Simulated and measured radiation patterns (in gain). (a) 860 MHz, (b) 910 MHz, (c) 960 MHz.

a maximum difference of approximately 1.3 dBi observed at 910 MHz. This difference is probably due to the antenna support structure, which is not accounted for in the simulation model. In terms of backward radiation, the antenna achieves high measured F/B ratios of 30.9 dB, 31 dB, and 24.09 dB at the three considered frequencies 860 MHz, 910 MHz, and 960 MHz, respectively. The simulated and measured radiation patterns (E and H-plane) at 860, 910, and 960 MHz are plotted in Fig. 9. It can be noticed that the measured patterns agree well with the simulated ones, with some slight shifts in the E-plane at 960 MHz. The U-slot antenna over AMC reflector exhibits a relatively stable directional radiation pattern with measured gains of 7.65 dBi, 7.54 dBi, and 4.80 dBi at 860 MHz, 910 MHz, and 960 MHz, respectively.

The size and characteristics of the proposed AMC backed antenna are compared to those of state-of-the-art UHF-RFID reader antennas in Table 1. The proposed structure shows lower profile except for the design in [26] and higher F/B ratio than the listed works. In summary, the proposed antenna demonstrates attractive performances. It fulfills the required specifications including size, range, gain, and F/B ratio, making it well suited for applications in RFID systems.

4. CONCLUSION

In this paper, a low profile probe-fed U-slot patch antenna loaded with a slotted AMC reflector is proposed for UHF-RFID applications. The slotted AMC reflector, comprising 2×2 unit cells, is positioned at a distance of 0.03λ from the U-slot patch antenna. The prototype is fabricated and measured. The simulated and measured results are in good agreement, validating the antenna's performance across the entire UHF-RFID band (860–960 MHz). The proposed AMC reflector-based antenna features a measured realized gain above 5 dBi with a high F/B ratio above 24 dB across the full UHF-RFID band. The obtained results are compared to similar state-of-the-art works, demonstrating highly attractive performances in terms of profile height, gain, and F/B ratio behavior. These characteristics make it well suited for UHF-RFID applications. Supplementary tests in real environment are planned to further validate the proposed RFID design.

ACKNOWLEDGEMENT

The authors thank Pierre Lemaître Auger, Dahmane Allane and Smail Tedjini for helping with antenna testing.

REFERENCES

[1] Li, J., H. Liu, S. Zhang, M. Luo, Y. Zhang, and S. He, "A wideband single-fed, circularly-polarized patch antenna with enhanced axial ratio bandwidth for UHF RFID reader applications," *IEEE Access*, Vol. 6, 55 883–55 892, 2018.

[2] Wu, C., X. Liu, C. Liao, W. Zhang, X. Liu, C. Liu, H. Cao, K.-W. Tam, S. Huang, and Y. Zhang, "A broadband miniaturized circularly polarized microstrip patch antenna for UHF RFID reader," in *2023 Cross Strait Radio Science and Wireless Technology Conference (CSRSWTC)*, 1–2, Guilin, China, 2023.

[3] Latrach, M. and I. M. D. Saiful, "High-directivity and circularly polarized compact patch antenna for UHF RFID reader devices," in *ITM Web of Conferences*, Vol. 48, 01012, 2022.

[4] Jung, Y.-K. and B. Lee, "Dual-band circularly polarized microstrip RFID reader antenna using metamaterial branch-line coupler," *IEEE Transactions on Antennas and Propagation*, Vol. 60, No. 2, 786–791, 2011.

[5] Fang, D.-G., *Antenna Theory and Microstrip Antennas*, 311, CRC Press, Boca Raton, 2017.

[6] Chen, Z. N., X. Qing, and H. L. Chung, "A universal UHF RFID reader antenna," *IEEE Transactions on Microwave Theory and Techniques*, Vol. 57, No. 5, 1275–1282, 2009.

[7] Nestoros, M., M. A. Christou, and A. C. Polycarpou, "Design of wideband, circularly polarized patch antennas for RFID applications in the FCC/ETSI UHF bands," *Progress In Electromagnetics Research C*, Vol. 78, 115–127, 2017.

[8] Qing, X., Nasimuddin, and Z. N. Chen, "A wideband circularly polarized stacked slotted microstrip patch antenna," *IEEE Antennas and Propagation Magazine*, Vol. 55, No. 6, 84–99, 2013.

[9] Kovitz, J. M. and Y. Rahmat-Samii, "Using thick substrates and capacitive probe compensation to enhance the bandwidth of traditional CP patch antennas," *IEEE Transactions on Antennas and Propagation*, Vol. 62, No. 10, 4970–4979, 2014.

[10] Lu, H.-X., F. Liu, M. Su, and Y.-A. Liu, "Design and analysis of wideband U-slot patch antenna with U-shaped parasitic elements," *International Journal of RF and Microwave Computer-Aided Engineering*, Vol. 28, No. 2, e21202, 2018.

[11] Patel, A. K., S. Yadav, A. K. Pandey, and R. Singh, "A wideband rectangular and circular ring-shaped patch antenna with gap coupled meandered parasitic elements for wireless applications," *International Journal of RF and Microwave Computer-Aided Engineering*, Vol. 30, No. 1, e21992, 2020.

[12] Gupta, S., S. Patil, C. Dalela, and B. K. Kanaujia, "Analysis and design of inclined fractal defected ground-based circularly polarized antenna for CA-band applications," *International Journal of Microwave and Wireless Technologies*, Vol. 13, No. 4, 397–406, 2021.

[13] Yeh, C. H., Y. W. Hsu, and C. Y. D. Sim, "Equilateral triangular patch antenna for UHF RFID applications," *International Journal of RF and Microwave Computer-Aided Engineering*, Vol. 24, No. 5, 580–586, 2014.

[14] Konjunthes, S., W. Thaiwirot, and P. Akkaraekthalin, "A wideband circularly polarized stacked patch antenna with truncated corners ground plane for universal UHF RFID reader," in *2020 17th International Conference on Electrical Engineering/Electronics, Computer, Telecommunications and Information Technology (ECTI-CON)*, 84–87, Phuket, Thailand, 2020.

[15] Boumaaza, K., S. Hebib, Y. Bennani, and L. Mouffok, "Broadband U-Slot patch antenna for RFID-UHF reader," in *2019 International Conference on Advanced Electrical Engineering (ICAEE)*, 1–4, Algiers, Algeria, 2019.

[16] Jamali Arand, A. and B. A. Arand, "Performance enhancement of microstrip antenna using artificial magnetic conductor reflection phase characteristics," *International Journal of RF and Microwave Computer-Aided Engineering*, Vol. 31, No. 8, e22705, 2021.

[17] Li, Y. and J. Chen, "Design of miniaturized high gain bowtie antenna," *IEEE Transactions on Antennas and Propagation*, Vol. 70, No. 1, 738–743, 2021.

[18] Salman, M. Z., M. Keerthana, R. Kajur, and A. Parameswaran, "Miniaturized slotted microstrip patch antenna using artificial magnetic conductor," in *2022 IEEE Wireless Antenna and Microwave Symposium (WAMS)*, 1–4, Rourkela, India, 2022.

[19] Jiang, Z., Z. Wang, L. Nie, X. Zhao, and S. Huang, "A low-profile ultrawideband slotted dipole antenna based on artificial magnetic conductor," *IEEE Antennas and Wireless Propagation Letters*, Vol. 21, No. 4, 671–675, 2022.

[20] Wu, R., S. Cao, Y. Liu, and S. Cai, "A wideband low-profile dual-polarized antenna based on a metasurface," *Electronics*, Vol. 12, No. 23, 4739, 2023.

[21] Sievenpiper, D., L. Zhang, R. F. J. Broas, N. G. Alexopolous, and E. Yablonovitch, "High-impedance electromagnetic surfaces with a forbidden frequency band," *IEEE Transactions on Microwave Theory and Techniques*, Vol. 47, No. 11, 2059–2074, 1999.

[22] Sarkar, S. and B. Gupta, "A dual-band circularly polarized antenna with a dual-band AMC reflector for RFID readers," *IEEE Antennas and Wireless Propagation Letters*, Vol. 19, No. 5, 796–800, 2020.

[23] Xu, J., X. He, and D. Ding, "An UHF RFID reader antenna with high front-to-back ratio," in *2023 IEEE 11th Asia-Pacific Conference on Antennas and Propagation (APCAP)*, 1–2, IEEE, 2023.

[24] Xu, R., J. Liu, K. Wei, W. Hu, Z.-J. Xing, J.-Y. Li, and S. S. Gao, "Dual-band circularly polarized antenna with two pairs of crossed-dipoles for RFID reader," *IEEE Transactions on Antennas and Propagation*, Vol. 69, No. 12, 8194–8203, 2021.

[25] Gupta, G., B. P. Singh, A. Bal, D. Kedia, and A. R. Harish, "Orientation detection using passive UHF RFID technology," *IEEE Antennas and Propagation Magazine*, Vol. 56, No. 6, 221–237, 2014.

[26] Wang, Z. and Y. Dong, "Miniaturized RFID reader antennas based on CRLH negative order resonance," *IEEE Transactions on Antennas and Propagation*, Vol. 68, No. 2, 683–696, 2019.